*Traffic 2002; **3**: 666–677*
Blackwell Munksgaard

ISSN 1398-9219

Pallidin is a Component of a Multi-Protein Complex Involved in the Biogenesis of Lysosome-related Organelles

Kengo Moriyama and Juan S. Bonifacino*

Cell Biology and Metabolism Branch, National Institute of Child Health and Human Development, National Institutes of Health, Bethesda, MD 20892, USA
** Corresponding author: Juan S. Bonifacino, juan@helix.nih.gov*

The Hermansky–Pudlak syndrome defines a group of genetic disorders characterized by defective lysosome-related organelles such as melanosomes and platelet dense bodies. Hermansky–Pudlak syndrome can be caused by mutations of at least four genes in humans and 15 genes in mice. One of these genes is mutated in the pallid mouse strain and encodes a novel protein named pallidin (L. Huang, Y. M. Kuo and J. Gitschier, Nat Genet 1999; 23:329–332). Pallidin has no homology to any other known protein and no recognizable functional motifs. We have conducted a biochemical characterization of human pallidin using a newly developed polyclonal antibody. We show that pallidin is a ubiquitously expressed ~25 kDa protein found both in the cytosol and peripherally associated to membranes. Sedimentation velocity analyses show that native pallidin has a sedimentation coefficient of ~5.1 S, much larger than expected from the molecular mass of the pallidin polypeptide. In line with this observation, cosedimentation and coprecipitation analyses reveal that pallidin is part of a hetero-oligomeric complex. One of the subunits of this complex is the product of another Hermansky–Pudlak syndrome gene, muted. Fibroblasts derived from the muted mouse strain exhibit reduced levels of pallidin, suggesting that the absence of the muted protein destabilizes pallidin. These observations indicate that pallidin is a subunit of a novel multi-protein complex involved in the biogenesis of lysosome-related organelles.

Key words: adaptors, BLOC-1, Hermansky–Pudlak syndrome, lysosomes, melanosomes, pigmentation

Received 28 May 2002, revised and accepted for publication 6 June 2002

The Hermansky–Pudlak syndrome (HPS) is a genetically heterogeneous disorder characterized by defective lysosome-related organelles such as melanosomes and platelet dense bodies (1–3). To date, mutations in any of four genes termed *HPS1–HPS4* have been demonstrated to cause HPS in humans. *HPS2* (*AP3B1*) encodes the β3A subunit of adaptor protein complex 3 (AP-3) (4,5), one of four adaptor protein (AP) complexes involved in sorting integral membrane proteins in the endosomal–lysosomal system (6). *HPS1* (7), *HPS3* (8) and *HPS4* (9), on the other hand, encode proteins with no significant homology to other proteins and no recognizable sequence motifs. Some HPS patients do not have mutations in any of these genes, indicating that additional *HPS* genes remain to be identified.

Likely candidates for novel *HPS* genes are the orthologs of genes that are mutated in 15 mouse strains exhibiting melanosome and platelet dense body defects similar to those of human HPS (10). Indeed, the products of the *HPS1–HPS4* genes are orthologous to those mutated in the pale ear (11,12), pearl (13), cocoa (14) and light ear (9) mouse strains, respectively. The genes mutated in four additional mouse models of HPS, mocha (15), gunmetal (16), pallid (17), and muted (18), have been recently identified. The mocha gene encodes another subunit of AP-3, δ-adaptin (15), while the gunmetal gene encodes a subunit of a Rab geranylgeranyltransferase that adds prenyl groups to the carboxyl terminus of Rab GTPases (16). The products of the pallid and muted genes exhibit no homology to other proteins. AP-3 (6) and Rabs (19) are known components of the vesicle trafficking machinery, emphasizing the importance of vesicular trafficking events for melanosome and platelet dense body biogenesis. The fact that at least five other *HPS* gene products are novel proteins, however, suggests the existence of molecular processes that are specific to the biogenesis of melanosomes and platelet dense bodies. The roles of these novel proteins remain to be elucidated without the benefit of structural homologies that could point to their functions.

We have undertaken a biochemical approach to characterize the properties of pallidin, the protein that is defective in the pallid mouse strain (17). Like other HPS mouse models, pallid mice exhibit hypopigmentation of the coat and eyes due to abnormal melanosomes, as well as prolonged bleeding due to abnormal platelet dense bodies (10). In addition, pallid mice develop lung fibrosis that results in a shortened lifespan (20). Finally, these mice exhibit defects in otolith formation that lead to balance abnormalities (10). Cloning of the pallid gene revealed that mouse pallidin is a novel protein of 172 amino acid residues (17). Two-hybrid and immunoprecipitation assays showed that pallidin interacts with syntaxin 13, a t-SNARE protein involved in vesicle docking and fusion (17). This interaction suggested that pallidin could be involved in a vesicle fusion step of melanosome and platelet dense body biogenesis. Other biochemical properties of pallidin, however, have not been characterized. Here, we present evi-

dence that human pallidin is a widely expressed, ~25 kDa protein that exists as a subunit of a multi-protein complex. This complex also comprises the ~25 kDa protein product of the muted gene and three other proteins with molecular masses of ~32 kDa, ~20 kDa and ~15 kDa. We propose that pallidin fulfills its role in melanosome and platelet dense body biogenesis as part of this complex.

Results

Identification of human pallidin

A cDNA encoding human pallidin was identified based on its homology to mouse pallidin (17). The human cDNA encodes a protein of 172 amino acids that is 86% identical at the amino acid level to the mouse protein (17). Partial sequences encoding pallidin orthologs were identified in the rat (AC111203.1) and Japanese puffer fish (*Fugu rubripes*) (scaffold 8243) genomes. A more distantly related protein in the fruit fly, *Drosophila melanogaster* (AE003544), also exhibits some homology to pallidin from other species. None of these proteins displays homology to other known proteins. Secondary structure analyses, however, predict that they all have a similar secondary structure, with an unstructured amino-terminal domain of 40–50 amino acids followed by a domain with high α-helical content and a high probability of forming coiled-coils. In the case of human pallidin, two segments of coiled-coils could be discerned between amino acids 60–100 and 109–172. Since coiled-coils often mediate protein–protein interactions (21), the structure of pallidin suggests that it could form complexes with other proteins.

To characterize the biochemical properties of human pallidin, we produced a rabbit polyclonal antibody to a GST–human-pallidin fusion protein. The antibody recognized a major ~25 kDa species in untransfected HeLa cells, as determined by immunoblotting (Figure 1A, lane 4, asterisk). The molecular mass of this protein was higher than the ~20 kDa predicted from its amino acid composition. Metabolic labeling with ^{32}P-orthophosphate revealed that the ~25 kDa protein was phosphorylated (Figure 2A). However, treatment of the ^{35}S-methionine-labeled ~25 kDa protein with alkaline phosphatase did not change the electrophoretic mobility of the protein (Figure 2B), even though it slightly decreased the mobility of the β3A subunit of AP-3, as previously reported (22). Alkaline phosphatase treatment also eliminated most labeling from a lysate of ^{32}P-orthophosphate-labeled HeLa cells (data not shown). Thus, the aberrant mobility of pallidin is not likely due to phosphorylation, but could be due to another post-translational modification or to the highly charged nature of the protein (17).

Several tests were performed to demonstrate the specificity of pallidin immunodetection. First, the ~25 kDa band was not detected using serum from a control rabbit (Figure 1A, lanes 1–3), or antibodies to the Myc (Figure 1A, lane 7) or HA (Figure 1A, lane 8) epitopes. Second, the anti-pallidin antiserum recognized transgenic Myc-pallidin (Figure 1A, lane 5) and HA-pallidin (Figure 1A, lane 6), which could be observed as additional bands of ~27 kDa, consistent with the expected molecular mass of the tagged proteins. Third, the ~25 kDa band could be observed in fibroblasts from C57BL

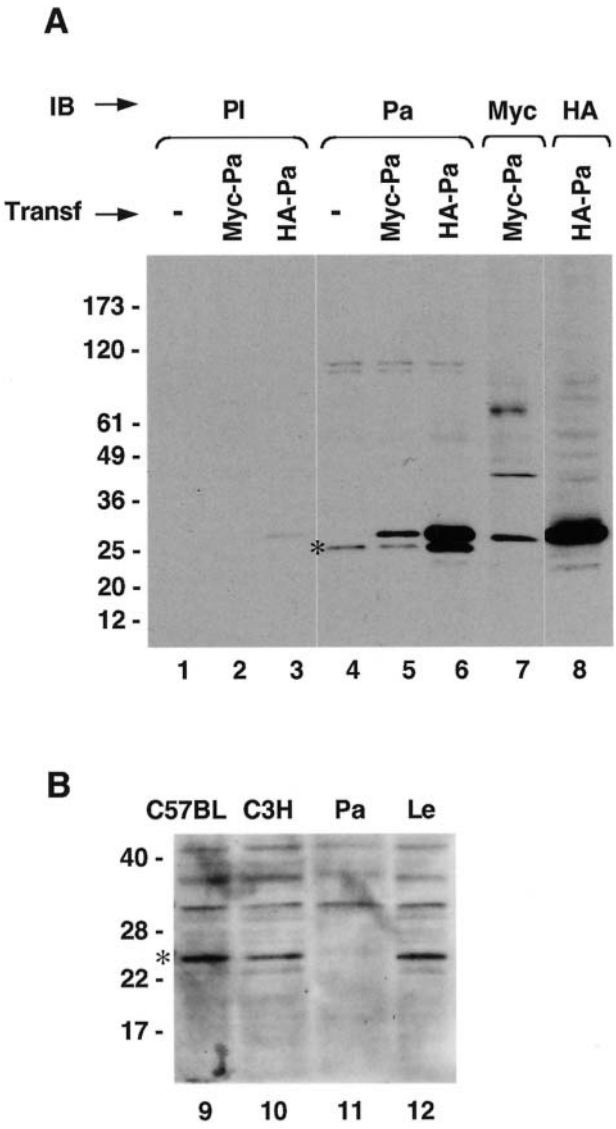

Figure 1: Identification of human pallidin using a new polyclonal antibody reagent. (A) Immunoblot analysis of untransfected HeLa cells (–) or HeLa cells transfected (Transf) with constructs encoding Myc-tagged pallidin (Myc-Pa) or HA-tagged pallidin (HA-Pa). Cells were analyzed by SDS-PAGE and immunoblotting (IB) with pre-immune serum (PI), anti-pallidin antiserum (Pa), or antibodies to the Myc or HA epitopes, as indicated in the figure. A ~25 kDa band corresponding to endogenous pallidin is indicated by an asterisk on lane 4. The positions of molecular mass markers (in kDa) are indicated on the left. (B) Lack of pallidin expression in fibroblasts from pallid mice. Fibroblasts in primary culture prepared from the wild-type mouse strains C57BL and C3H, and from the coat color mutant strains pallid (Pa) and light ear (Le) were analyzed for the presence of pallidin (asterisk) by SDS-PAGE and immunoblotting with anti-pallidin antiserum. The positions of molecular mass markers (in kDa) are indicated on the left. Notice the absence of the ~25 kDa pallidin band in the pallid fibroblasts (lane 11).

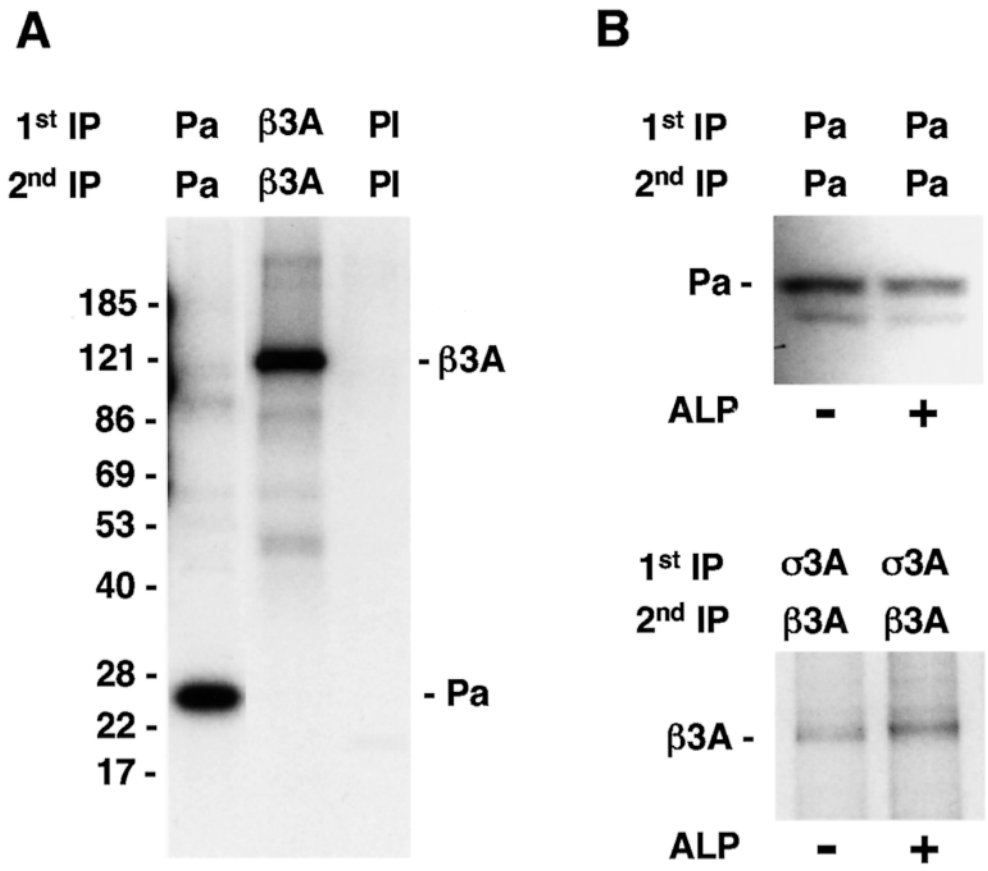

Figure 2: Human pallidin is a phosphorylated protein. (A) H4 cells were metabolically labeled for 3 h with ^{32}P-orthophosphate. Cells were extracted with 1% (w/v) Triton X-100, 50 mM Tris-HCl (pH 7.5), 0.3 M NaCl, 5 mM EDTA, and the extracts were subjected to immunoprecipitation recapture (1st IP−2nd IP, respectively) with antibodies to pallidin (Pa) or to the β3A subunit of AP-3, or with pre-immune serum (PI), as indicated in the figure. Immunoprecipitates were analyzed by SDS-PAGE and autoradiography. The positions of molecular mass markers (in kDa) are indicated on the left. The positions of ^{32}P-labeled pallidin and ^{32}P-labeled β3A subunit of AP-3 are indicated on the right. (B) Pallidin and the β3A subunit of AP-3 were isolated by immunoprecipitation recapture (1st IP−2nd IP, respectively) from H4 cells that were metabolically labeled with ^{35}S-methionine. The proteins were isolated with antibodies to pallidin (Pa) or the σ3A and β3A subunits of AP-3, as indicated in the figure. Immunoprecipitates were then either mock-treated (−) or treated with alkaline phosphatase (ALP, +) before analysis by SDS-PAGE and fluorography. The positions of pallidin (Pa) and β3A are indicated on the left.

and C3H wild-type mice and light ear mutant mice, but not in fibroblasts from pallid mice (Figure 1B). Finally, immunodetection of the ~25 kDa band from HeLa cells could be competed with excess GST-pallidin (data not shown). Therefore, by all of these criteria, the ~25 kDa species corresponds to endogenous pallidin.

Expression of pallidin in different cells and organs

The availability of an antiserum to human pallidin allowed us to examine the expression of this protein by immunoblot analysis of various cell lines and organs. We found that pallidin was expressed in HeLa (human epithelial), MNT1 (human melanoma), HepG2 (human hepatoma), N-tera-2 (human teratocarcinoma), H4 (human neuroglioma), COS-1 (monkey fibroblastoid), M1 (human fibroblastoid) and RD4 (human rhabdomyosarcoma) cell lines (Figure 3). The highest expression levels were observed in H4 cells. We could not detect pallidin in MDCK (dog epithelial), RBL (rat basophilic) and H35 (rat hepatoma) cells (Figure 3), but this could be due to a failure of the antiserum to recognize dog or rat pallidin. We did observe expression of pallidin in mouse liver, kidney and spleen, but low or undetectable levels in brain, lung and heart (Figure 3). These observations indicated that pallidin is widely expressed in mammalian cells and tissues, and that its expression is not restricted to cell types in which its absence results in overt phenotypes (e.g. melanocytes and megakaryocytes). This is consistent with the pattern of expression of other HPS gene products, which are also expressed ubiquitously. The fact that some cell lines (Figure 3), as well as fibroblasts from pallid mice (Figure 1B), do not express detectable levels of pallidin indicates that this protein is dispensable for cell viability and for most basic cell functions.

Pallidin exists in both cytosolic and membrane-bound pools

Most subsequent biochemical analyses of pallidin were performed on H4 cells because of the higher expression levels

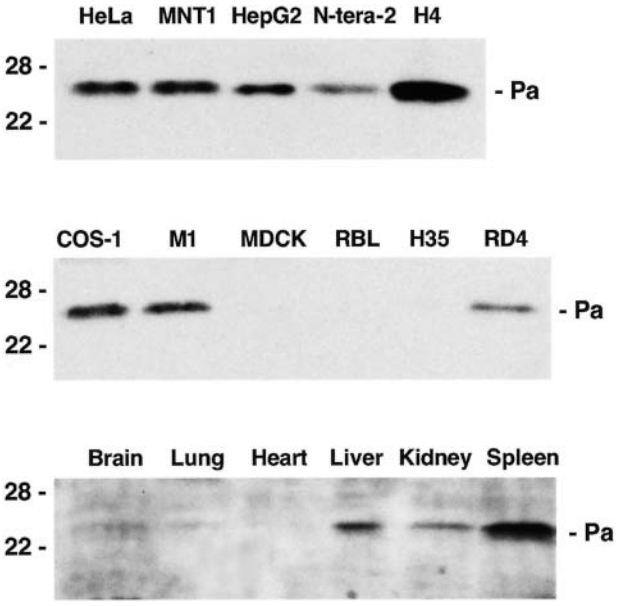

Figure 3: Expression of pallidin in different cell lines and organs. The expression of pallidin in the cell lines (top and middle panels) and mouse organs (bottom panel) indicated in the figure was analyzed by SDS-PAGE and immunoblotting using an antiserum to human pallidin. Samples were normalized for equal protein loads. Portions of the blots centered on the ~25 kDa pallidin are shown.

of pallidin in these cells (Figure 3). Upon cell lysis in 10 mM Tris-HCl (pH 7.5), 0.25 M sucrose, followed by ultracentrifugation, pallidin was found in both the membrane (M) and cytosolic (C) fractions (Figure 4A). Lysis in 10 mM HEPES, 0.15 M KCl, 1 mM EGTA, 0.5 mM $MgCl_2$, 1 mM dithiothreitol (DTT), on the other hand, rendered most of the protein cytosolic (Figure 4A). Subtraction of 0.15 M KCl from this solution prevented the loss of pallidin from the membrane fraction (Figure 4B). Thus, pallidin exists in both cytosolic and peripheral (i.e. salt-extractable) membrane-bound pools. The small amount of pallidin that was recovered in the membrane fraction upon lysis in the presence of 0.15 M KCl was very refractory to extraction with high salt and could only be dissociated with 0.2 M Na_2CO_3, pH 11.3. Thus, this pool appears to be more tightly bound to membranes or the cytoskeleton. This distribution of pallidin is reminiscent of that of other HPS gene products that cycle between the cytosol and membranes (23,24).

Pallidin sediments as large-sized species

To investigate the size of native pallidin, we analyzed extracts of various cell lines by sedimentation velocity analysis on sucrose gradients. The gradients were divided into 16 fractions, each of which was subjected to SDS-PAGE and immunoblotting with anti-pallidin antiserum. Interestingly, the bulk of pallidin peaked in fractions 7–8 (Figure 5, top three panels), which corresponds to a species with a sedimentation coefficient of ~5.1 S and a size larger than that of BSA (4.6 S, 69 kDa). The exact molecular mass of native pallidin could not be calculated from these experiments, however, because the shape and partial specific volume of pallidin are unknown. In any event, pallidin or HA-pallidin overexpressed by transfection into HeLa cells peaked in fractions 3–4 (Figure 5, bottom two panels), as would be expected for a ~25 kDa species. The larger size of endogenous pallidin relative to overexpressed pallidin suggested that endogenous pallidin was part of a complex with other polypeptides.

Pallidin is a component of a multi-protein complex

We attempted to identify other proteins that assemble with pallidin by coprecipitation from extracts of ^{35}S-methionine-labeled H4 cells. Unfortunately, the immunoprecipitates had too much background to allow direct visualization of specifically coprecipitated proteins. To overcome this problem, the labeled cell extracts were sedimented on sucrose gradients, after which pallidin was immunoprecipitated from each gradient fraction. As previously observed by immunoblotting (Figure 5), ^{35}S-methionine-labeled pallidin peaked in fractions 7 and 8 (Figure 6A, upper panel, asterisk). Interestingly, we observed three other labeled species of ~32 kDa, ~20 kDa and ~15 kDa that both cosedimented and coprecipitated with pallidin (Figure 6A, dots). These species appeared specific, as they were not observed in immunoprecipitations with preimmune serum (Figure 6A, lower panel). All four bands were competed by the addition of excess GST-pallidin or His_{10}-pallidin to the immunoprecipitation mixtures, and could be immunoprecipitated with affinity-purified antibodies to pallidin (data not shown), further demonstrating the specificity of the bands. Immunoprecipitation recapture analysis of fractions 7 and 8 with anti-pallidin antiserum resulted in the isolation of the ~25 kDa pallidin and a minor ~23 kDa species that was often observed in immunoprecipitates of denatured pallidin, but not the ~32 kDa, ~20 kDa and ~15 kDa species (Figure 6B). These observations thus confirmed that pallidin is part of a hetero-oligomeric complex. The presence of many nonspecific bands in the upper part of the fluorograms, even after fractionation on the sucrose gradients (Figure 6A,B), precluded the identification of larger proteins that could be part of the pallidin complex.

Analysis of the association of pallidin with other proteins

Because mutations in pallidin result in phenotypes similar to those of mutations in genes encoding AP-3 subunits or the HPS1 protein, it was of interest to examine whether pallidin interacts with these proteins. To this end, H4 cells were metabolically labeled with ^{35}S-methionine for 6 hr and solubilized with a buffer containing 1% (w/v) Triton X-100. The extracts were subjected to immunoprecipitation recapture using combinations of antibodies to pallidin, AP-3 and the HPS1 protein. We observed that, although the antibodies recognized the corresponding antigens, pallidin did not coprecipitate with either AP-3 (Figure 7A) or the HPS1 protein (Figure 7B). In addition, analyses of fibroblasts from wild-type and pallid mutant mice by immunofluorescence microscopy demonstrated that the absence of pallidin does not affect the distribution of AP-3 within cells (data not shown). Furthermore, overexpression of pallidin also failed to affect the distribution

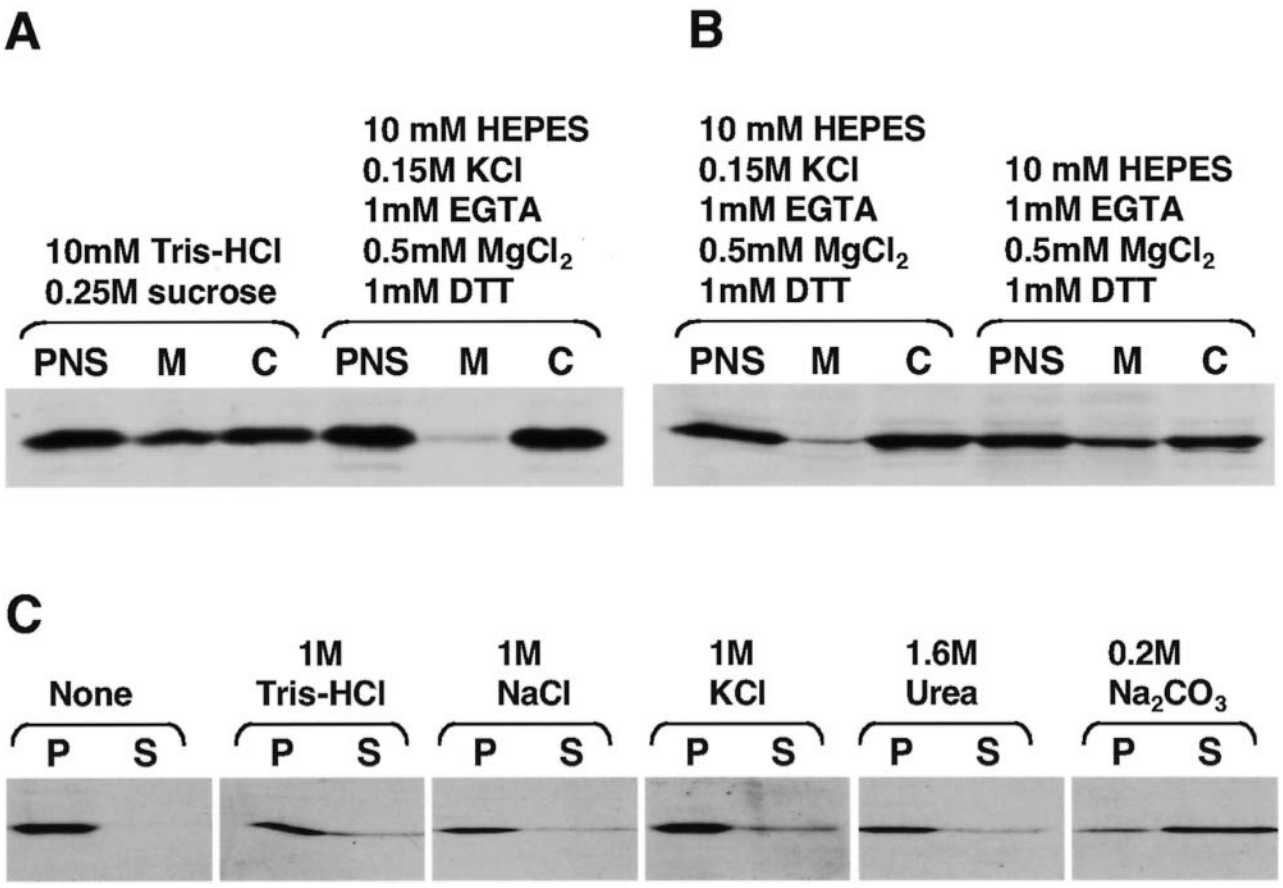

Figure 4: Analysis of the association of human pallidin with membranes. (A, B) H4 cells were lysed in the buffers indicated on top. A postnuclear supernatant (PNS) was fractionated into membrane (M) and cytosol (C) fractions. (C) The membrane fraction obtained after lysis in 10 mM HEPES, 0.15 M KCl, 1 mM EGTA, 0.5 mM $MgCl_2$, 1 mM DTT was resuspended in the solutions indicated in the figure. 1 M Tris-HCl and 0.2 M Na_2CO_3 were adjusted to pH 7.5 and 11.3, respectively. The suspensions were centrifuged for 1 h at 100 000 × g, yielding pellet (P) and supernatant (S) fractions. All samples were analyzed by SDS-PAGE and immunoblotting with antiserum to pallidin. Portions of the blots centered on the ~25 kDa pallidin are shown.

of AP-3 (data not shown). Together with previous findings (22), these observations suggest that pallidin, AP-3 and the HPS1 protein function at different steps of the biogenesis of lysosome-related organelles.

Mutations in the muted gene also result in a phenotype similar to that of the pallid mouse (18). Like pallidin, the muted protein is predicted to have an unstructured amino-terminal domain and a carboxyl-terminal coiled-coil domain. Immunoprecipitation recapture analyses revealed that a ~25 kDa species corresponding to the muted protein coprecipitated with pallidin (Figure 7C). Like pallidin, the muted protein could not be recaptured from immunoprecipitates performed with preimmune serum or with antibodies to the σ3 subunit of AP-3 or the HPS1 protein (Figure 7C). Sedimentation velocity analyses revealed that the muted protein from H4 cells peaked in fractions 7 and 8 (Figure 8A), just like pallidin (Figures 5 and 6). These observations indicated that the muted protein is part of a complex with pallidin.

The failure to synthesize one subunit of a multi-protein complex often results in the degradation of the other subunits (25), as is the case with AP-3 subunits in HPS2 patients (4) and the pearl mouse (26). This prompted us to test for the levels and size of native pallidin in fibroblasts in primary cultures prepared from several mouse HPS models. This was accomplished by sedimentation on sucrose gradients and immunoblotting. Interestingly, normal levels of pallidin peaking in fractions 7 and 8 were observed in samples from mocha, cocoa, light ear, and ruby eye-2 mice (Figure 8B). In contrast, no pallidin could be detected in fractions 7 and 8 of samples from pallid and muted fibroblasts (Figure 8B). This strongly suggests that the absence of the muted protein results in destabilization of pallidin. Strikingly, pallidin levels were likewise reduced or undetectable in fibroblasts from reduced pigmentation and cappuccino mice (Figure 8B), raising the possibility that the products of the corresponding genes could also be components of the pallidin complex.

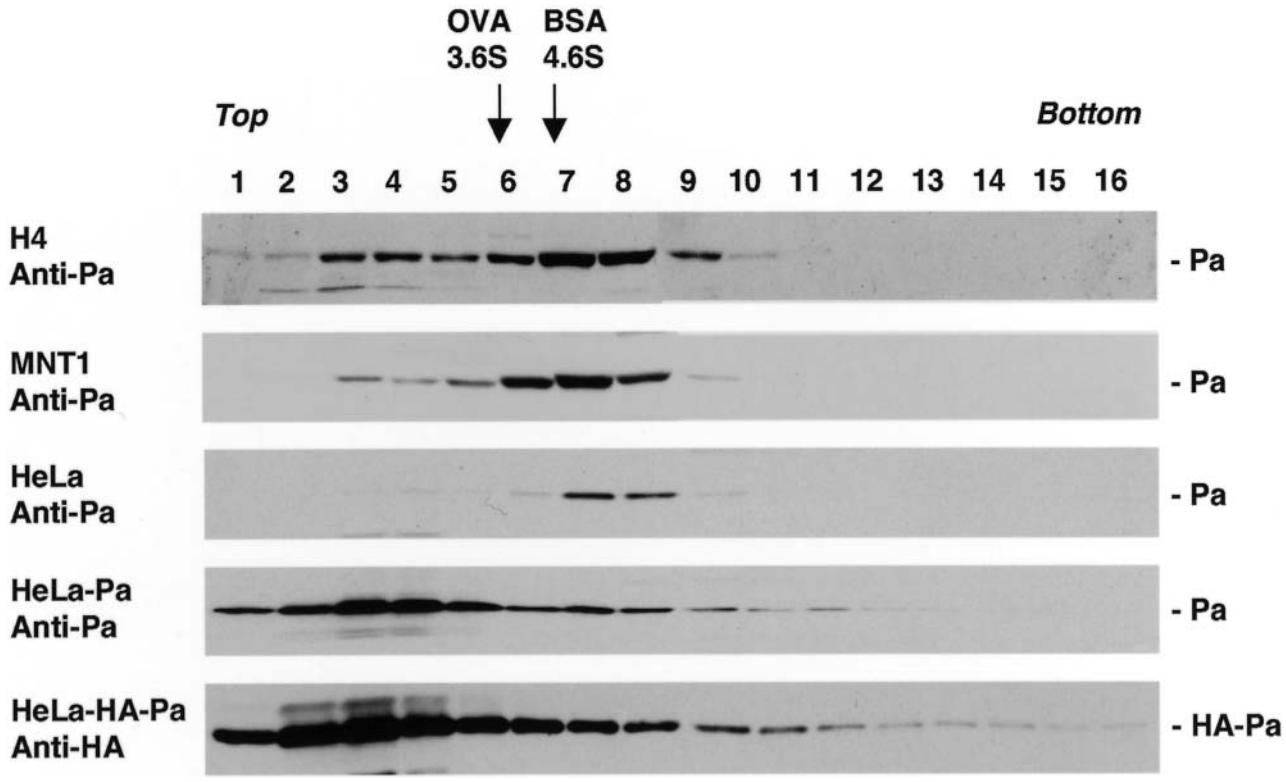

Figure 5: Sedimentation velocity analysis of native human pallidin. Untransfected H4, MNT1, or HeLa cells, or from HeLa cells transfected with constructs encoding human pallidin (Pa) or HA-pallidin (HA-Pa) were extracted with 20 mM HEPES buffer (pH 7.4), 0.15 M NaCl, 0.05% (w/v) Triton X-100, and analyzed by sedimentation velocity on 2–15% (w/v) sucrose gradients. Gradients were divided into 16 fractions that were analyzed by SDS-PAGE and immunoblotting with antibodies to human pallidin or to the HA epitope, as indicated in the figure. The positions of standard proteins, ovalbumin (OVA) and bovine serum albumin (BSA), on the sucrose gradients are indicated ($s_{20,w}$-values given in Svedberg units). Notice the faster sedimentation of endogenous pallidin (top three panels) relative to the transgenic pallidins (bottom two panels), indicative of the larger size of the endogenous protein.

Pallidin self-association and interaction with syntaxin 13

Pallidin has been reported to interact with syntaxin 13 (17), a membrane-bound target SNARE (t-SNARE) (27). Using the yeast two-hybrid system, we confirmed that pallidin interacts with syntaxin 13, specifically through its coiled-coil domain (Pa 60–172, Figure 9B). In the course of these experiments, we found that pallidin interacted even more strongly with itself, also via its coiled-coil domain (Figure 9B). This observation raises the possibility that the pallidin complex could have more than one copy of pallidin. Alternatively, pallidin–pallidin interactions could mediate polymerization of the pallidin complex, in a manner analogous to the polymerization of clathrin triskelia via the clathrin heavy chains (28).

Discussion

Melanosomes and platelet dense bodies belong to a family of specialized cytoplasmic granules known as 'lysosome-related organelles' (3,29). This term was coined to reflect the fact that many of these organelles contain both some lysosomal proteins and granule-specific molecules that are responsible for their non-degradative functions. Like lysosomes, these organelles are thought to originate by vesicular transport from the trans-Golgi network (TGN) and endosomes. At some point, however, their biogenetic pathways must diverge, as it is becoming increasingly clear that some cells possess separate lysosomes and lysosome-related organelles (30).

The study of HPS patients and mouse models of HPS is beginning to provide insights into the molecular machinery specific to the biogenesis of lysosome-related organelles.

To date, eight genes have been identified that, when mutated, cause HPS in humans or mice. Two of the known genes encode the δ and β3A subunits of the heterotetrameric AP-3 complex (4,13,15). Mutations in this complex result in increased trafficking of lysosomal membrane proteins such as CD63, lamp-1, lamp-2, and limp-II via the plasma membrane in fibroblasts (4,24,31,32) and impaired transport of tyrosinase to premelanosomes in melanocytic cell lines (33). These observations are consistent with the notion that AP-3 plays a role in sorting integral membrane proteins to both lysosomes and lysosome-related organelles. One mouse HPS gene (i.e. gunmetal) encodes a Rab geranylgeranyltransferase subunit (16), while five other genes (i.e. the pale

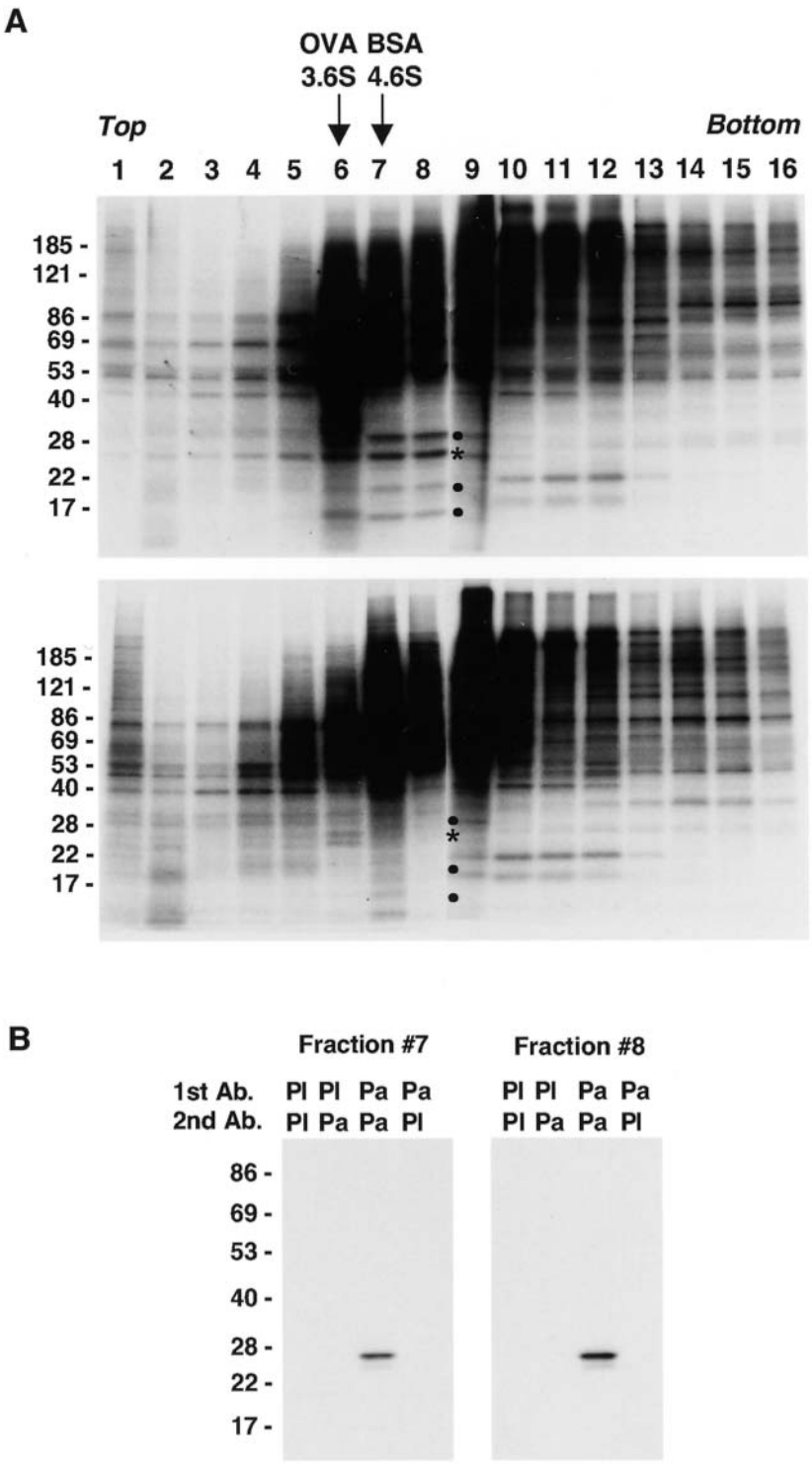

Figure 6: Identification of proteins that cosediment and coprecipitate with human pallidin. (A) H4 cells were metabolically labeled with ^{35}S-methionine for 6 h and extracted with 20 mM HEPES buffer (pH 7.4), 0.15 M NaCl, 0.05% (w/v) Triton X-100. The cell extracts were subjected to sedimentation on 2–15% (w/v) sucrose gradients. Sixteen gradient fractions were analyzed by immunoprecipitation with antiserum to pallidin (top panel) or pre-immune serum (bottom panel). Immunoprecipitates were resolved by SDS-PAGE and fluorography. In addition to the ~25 kDa pallidin (asterisk), notice the presence of species of ~32 kDa, ~20 kDa, and ~15 kDa (dots) that both cosediment and coprecipitate with pallidin. (B) Fractions 7 and 8 from an experiment similar to that described in (A) were subjected to immunoprecipitation recapture with various combinations of pre-immune serum (PI) and antiserum to pallidin (Pa). Notice the presence of only the ~25 kDa pallidin and a minor ~23 kDa species, and the absence of the other pallidin-associated proteins, in the immunoprecipitates. The positions of molecular mass markers (in kDa) are indicated on the left of each panel.

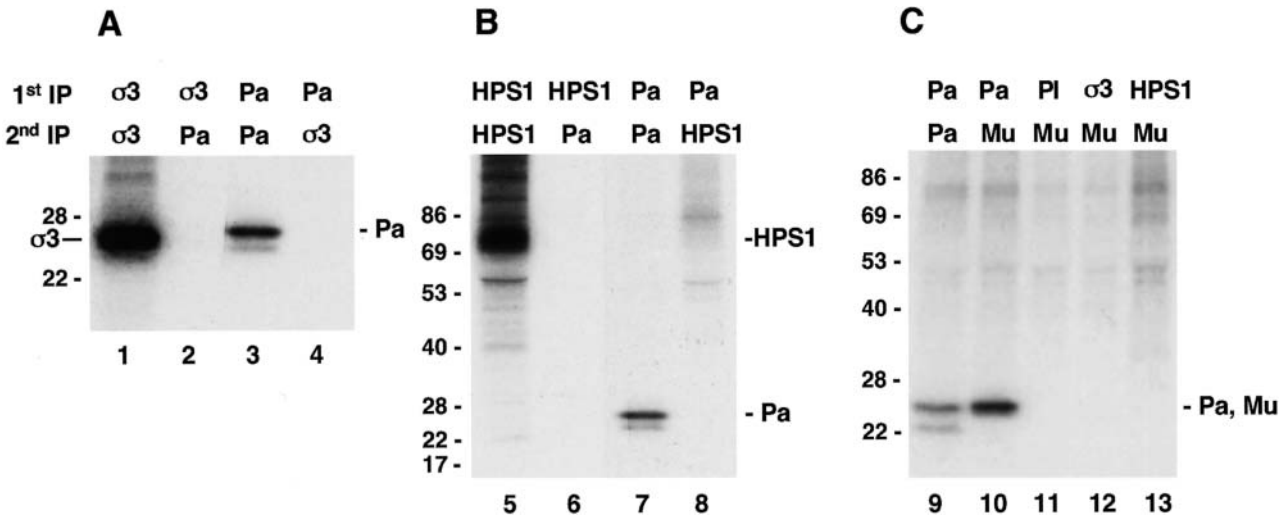

Figure 7: Analysis of the association of pallidin with the products of other HPS genes. (A–C) H4 cells were metabolically labeled with ^{35}S-methionine for 6 h and extracted with 1% (w/v) Triton X-100, 50 mM Tris-HCl (pH 7.5), 0.3 M NaCl, 5 mM EDTA. Cell extracts were subjected to immunoprecipitation recapture with the combinations of antibodies to human pallidin (Pa), the σ3 subunit of the AP-3 complex, the HPS1 protein, and the muted protein (Mu), indicated in the figure. The positions of molecular mass markers (in kDa) are indicated on the left of each panel.

ear/*HPS1*, light ear/*HPS4*, cocoa/*HPS3*, pallid, and muted) encode proteins that are unrelated to any other known proteins (7–9,11,12,14,17,18). Mutations in these genes have no detectable effect on the trafficking of lysosomal integral membrane proteins in fibroblasts (24), suggesting that they mediate events specific to the biogenesis of lysosome-related organelles.

It has been hypothesized that some of the novel HPS gene products could be components of multi-protein complexes. The pale ear/HPS1 protein, for example, has been shown to be absent from light ear/HPS4 fibroblasts, leading to the proposal that these proteins interact as part of a complex (9). In support of this notion, mice homozygous for mutations in both of these genes have the same phenotype as mice homozygous for mutations in either gene (10). Biochemical evidence for the existence of such a complex, however, still remains to be obtained.

Here we present evidence that two other novel HPS gene products, the ~25 kDa pallidin and muted proteins, are subunits of another multi-protein complex. This was demonstrated by both coprecipitation and cosedimentation. The pallidin complex is distinct from the putative pale ear/HPS1–light ear/HPS4 protein complex and the AP-3 complex, as pallidin does not coprecipitate with subunits of the latter two complexes. Instead, the pallidin complex appears to contain additional proteins. Among these are proteins with molecular masses of ~32 kDa, ~20 kDa and ~15 kDa. None of these proteins exhibited immunologic cross-reactivity with pallidin and may therefore be distinct from pallidin. The high background in the upper part of the gels precluded us from determining the presence of other pallidin-associated proteins of higher molecular mass. We speculate that the pallidin-associated proteins could be encoded by some of the HPS genes that remain to be cloned. In this regard, it is intriguing that pallidin seems to be absent from fibroblasts from the reduced pigmentation and cappuccino mice, two other models of HPS. In fact, pallid, muted and cappuccino are three of four HPS mouse models (the fourth being mocha) that exhibit the most severe pigmentation defect, together with otolith defects (34). Once the reduced pigmentation and cappuccino genes are cloned, it will be of interest to determine whether their protein products are components of the pallidin complex.

At present, we can only speculate as to the possible function of the pallidin complex. As discussed above, no defects in sorting of lysosomal membrane proteins have yet been detected in pallid or muted fibroblasts (24). Similarly, we did not observe any difference in the distribution of Golgi and endosomal markers in pallid and muted fibroblasts (data not shown). Other processes in which the pallidin complex could participate are the translocation of transport intermediates or the tethering or fusion of the intermediates with acceptor organelles. It is noteworthy that both pallidin and the muted protein are not homologous to any other proteins, contain coiled-coil regions and are part of a multi-protein complex. These are precisely the characteristics of components of several tethering complexes that participate in specific vesicle fusion events (35–39). Vesicular transport to lysosome-related organelles most likely requires a specific tethering complex, for which the pallidin complex is an attractive candidate. It is perhaps in this context that the interaction between pallidin and syntaxin 13 fulfills a physiological role, as previously proposed for interactions between other tethering complexes and SNAREs (40).

While this manuscript was in preparation, another study describing a multi-protein complex containing pallidin and the muted protein was published online (41). The authors of that

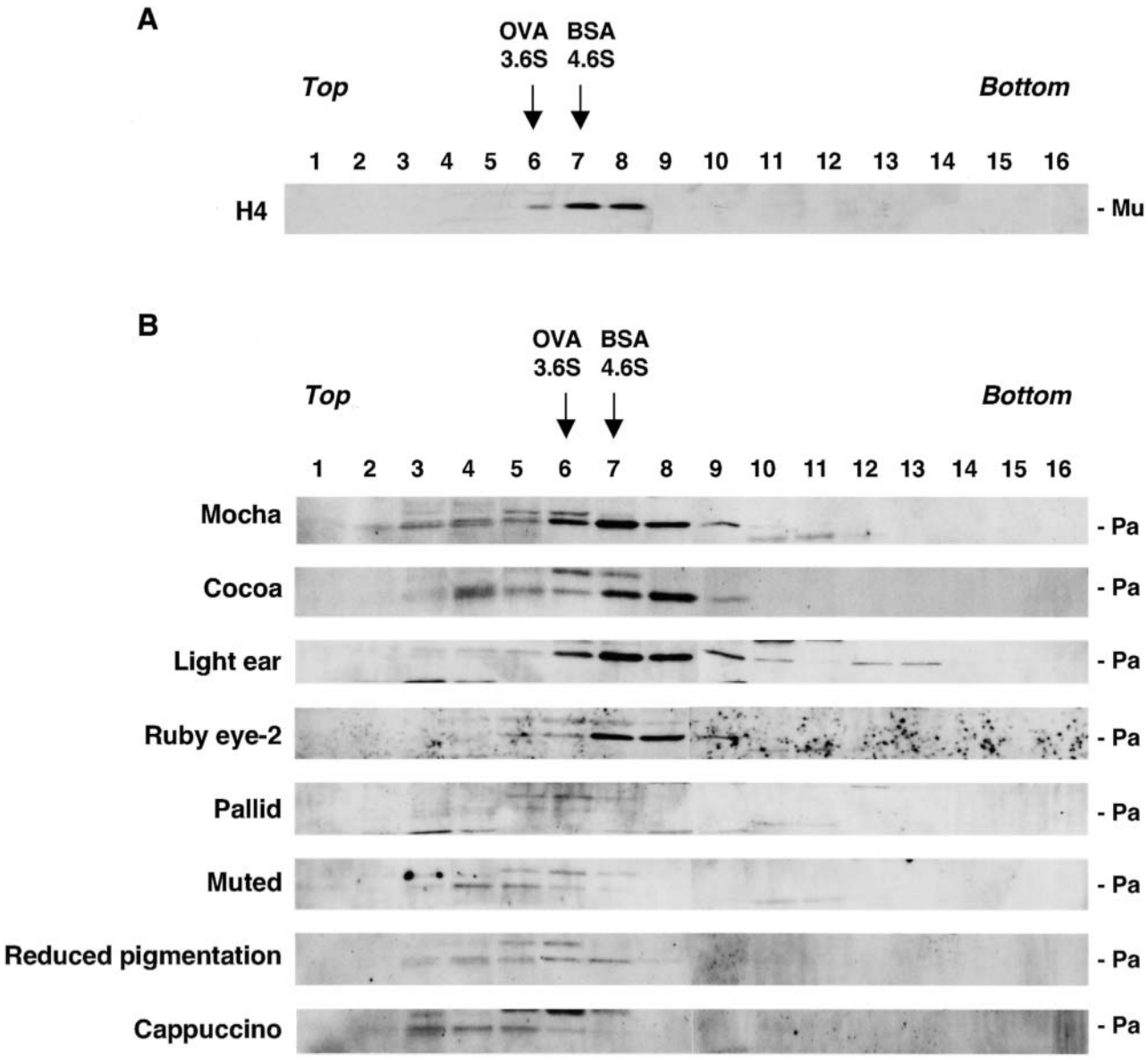

Figure 8: Cosedimentation of the muted and pallidin proteins. (A) H4 cells were extracted with 20 mM HEPES buffer (pH 7.4), 0.15 M NaCl, 0.05% (w/v) Triton X-100 and the extract was subjected to sedimentation on a 2–15% (w/v) sucrose gradient. Sixteen gradient fractions were analyzed by SDS-PAGE and immunoblotting with antiserum to the muted protein. The positions of standard proteins, ovalbumin (OVA) and bovine serum albumin (BSA), on the sucrose gradients are indicated ($s_{20,w}$-values given in Svedberg units). (B) Fibroblasts derived from the mutant mice indicated on the left were extracted with 20 mM HEPES buffer (pH 7.4), 0.15 M NaCl, 0.05% (w/v) Triton X-100 and the extract were analyzed by sucrose gradient centrifugation and immunoblotting as described. Pallidin (Pa) was detected by immunoblotting with anti-pallidin antiserum. Notice the absence of pallidin in samples from pallid, muted, reduced pigmentation and cappuccino fibroblasts. Portions of the blots centered on the ~25 kDa muted protein (Mu) and pallidin (Pa) are shown.

study named the complex, BLOC-1 (for *B*iogenesis of *L*ysosome-related *O*rganelles *C*omplex 1), a name that we have decided to adopt for future reference to this complex.

Materials and Methods

DNA recombinant procedures

A construct encoding a GST–pallidin fusion protein was generated by PCR amplification of a cDNA encoding human pallidin, followed by in-frame cloning into the *EcoR*I-*Not*I sites of the pGEX-4T-1 vector (Amersham Pharmacia Biotech, Piscataway, NJ, USA). The same insert was cloned in-frame into the *EcoR*I site of the pGBT9 and the *EcoR*I-*Sal*I sites of the pGAD424 vectors (Clontech, Palo Alto, CA, USA) to fuse it to the GAL4 DNA binding domain (Gal4bd) and GAL4 transcription activation domain (GAL4ad), respectively. A construct encoding a His_{10}-tagged pallidin was generated by in-frame cloning human pallidin cDNA into the *EcoR*I-*Not*I sites of a modified version of the pET-28a(+) vector. This plasmid was used to transform *Escherichia coli* BL21 (DE3)pLysS (Novagen, Madison, WI, USA). The recombinant His_{10}-tagged pallidin was purified on Ni-NTA Agarose (Qiagen, Valencia, CA, USA). Epitope tagging at the amino-ter-

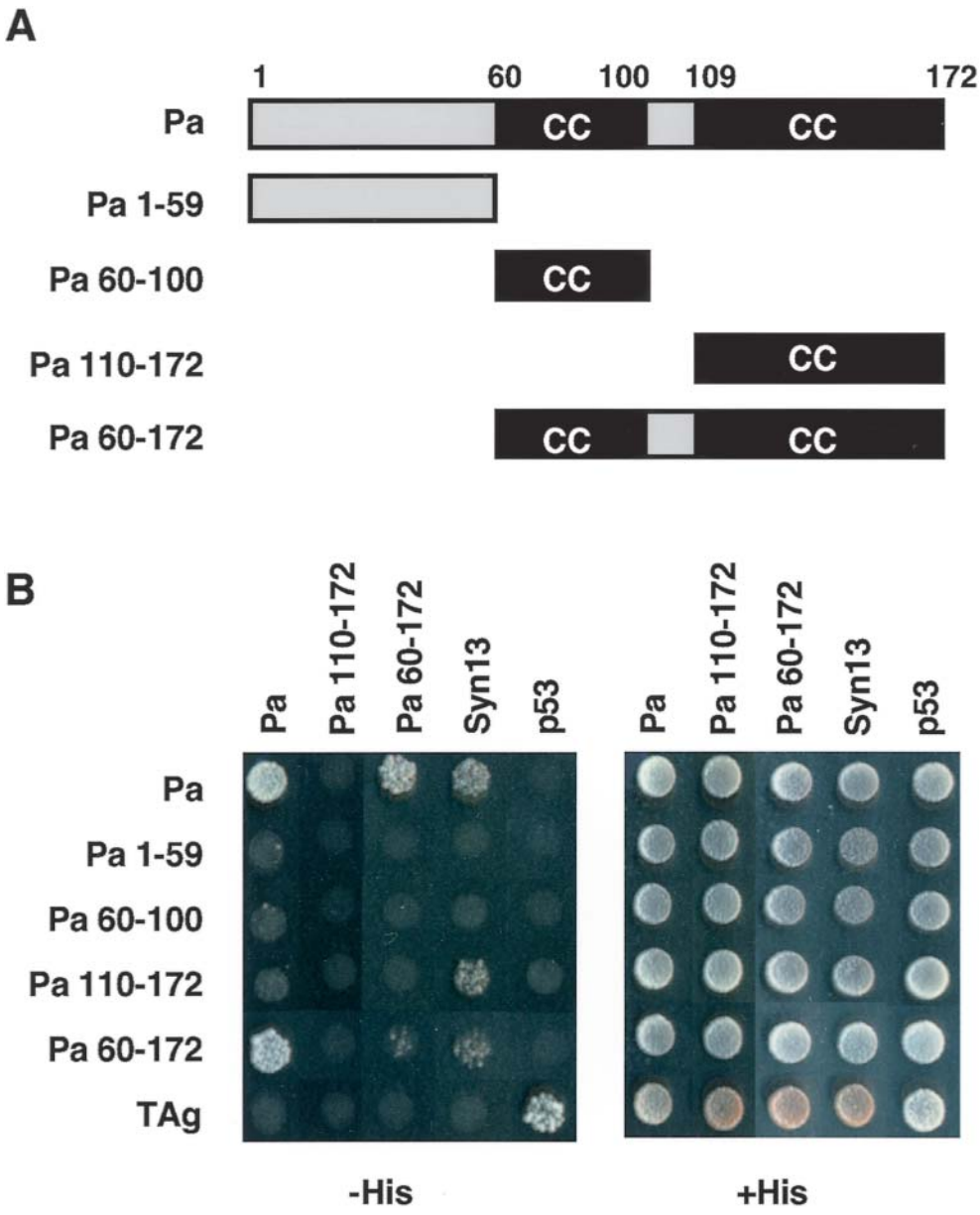

Figure 9: Self-association of human pallidin revealed by yeast two-hybrid assays. (A) Schematic representation of human pallidin (Pa) constructs fused to the GAL4bd. Amino acid numbers demarcating different segments of pallidin are indicated on top. Coiled-coil segments are indicated as CC. (B) Yeast cells were cotransformed with plasmids encoding GAL4ad fused to the constructs indicated on the left with GAL4bd fused to the constructs indicated on top. Fusions to the SV40 large T antigen (Tag) and mouse p53 were used as controls. Cotransformed cells were spotted onto histidine-deficient (−His) or histidine-containing (+His) plates and incubated at 30°C. Growth on −His plates is indicative of interactions.

minus of pallidin was performed by PCR amplification of the full-length pallidin cDNA using 5′-primers containing the nucleotide sequence coding for the Myc or HA epitopes. These products were cloned into the *EcoR*I-*Not*I sites of the mammalian expression vector pXS. Various mutants of pallidin for yeast two-hybrid analysis were generated by PCR-based mutagenesis. A construct encoding rat syntaxin 13 (27) was generated by PCR amplification, followed by in-frame cloning into the *EcoR*I-*Sal*I sites of the pGBT9 vector (Clontech).

Cells and antibodies

The generation of primary cultures of fibroblasts from mouse skin and the sources and culture conditions for the cell lines M1, HeLa, H4, COS-1, MDCK, RBL, HepG2, H35, RD4, MNT1, N-tera-2 and Jurkat have been described in previous reports (23,24,34). HeLa cells were transfected with Myc- or HA-tagged pallidin constructs using the FuGENE-6 reagent (Roche Molecular Biochemicals, Indianapolis, IN, USA). A polyclonal antiserum to human pallidin was raised by immunization of rabbits with a GST-

human pallidin fusion protein. An affinity-purified antibody was generated by affinity chromatography on His_{10}-tagged pallidin coupled to Affi-gel 10 (Bio-Rad, Hercules, CA, USA). A polyclonal antiserum to the muted protein was the kind gift of Richard Swank (Roswell Park Cancer Institute, Buffalo, NY, USA). The sources for all the other antibodies used in this study have been indicated elsewhere (23,24,34).

Biochemical procedures

Metabolic labeling of cultured cells with ^{35}S-methionine, extraction with Triton X-100, subcellular fractionation, sedimentation velocity on sucrose gradients, and immunoprecipitation recapture were performed as previously described (4,23). Metabolic labeling with ^{32}P-orthophosphate was carried out as previously described (22).

Electrophoresis and immunoblotting

SDS-PAGE was performed using the Laemmli system. ^{35}S-methionine-labeled samples were detected by fluorography and ^{32}P-orthophosphate-labeled samples by autoradiography. Electroblotting onto nitrocellulose membranes and incubation of the membranes with primary and secondary antibodies were performed as described previously (4). Horseradish peroxidase-conjugated secondary antibodies were detected using the ECL system (Amersham Pharmacia Biotech).

Alkaline phosphatase treatment

Pallidin was isolated from ^{35}S-methionine-labeled H4 cells by immunoprecipitation recapture (4). The immunoprecipitates were washed twice with dephosphorylation buffer consisting of 50 mM Tris-HCl (pH 8.5), 0.1 mM EDTA, and divided into two aliquots. One aliquot was treated with 0.2 units of calf intestinal alkaline phosphatase (Roche Molecular Biochemicals) for 2 h at 37 °C, while the other was mock-treated. Samples were analyzed by SDS-PAGE followed by fluorography.

Yeast two-hybrid analyses

The *Saccharomyces cerevisiae* strain AH109 (Clontech) was transformed by the lithium acetate method as described in the instructions for the MATCHMAKER two-hybrid kit (Clontech). AH109 transformants were resuspended in water to 0.1 OD_{600}/ml, and 5 µl was spotted on plates and incubated at 30 °C for 4–5 days.

Acknowledgments

We thank Richard Swank for generous gifts of reagents, Xiaolin Zhu for expert technical assistance, and other members of the Bonifacino lab for helpful advice.

References

1. Huizing M, Anikster Y, Gahl WA. Hermansky–Pudlak syndrome and related disorders of organelle formation. Traffic 2000;1:823–835.
2. Spritz RA. Hermansky–Pudlak syndrome and pale ear: melanosome-making for the millennium. Pigment Cell Res 2000;13:15–20.
3. Dell'Angelica EC, Mullins C, Caplan S, Bonifacino JS. Lysosome-related organelles. FASEB J 2000;14:1265–1278.
4. Dell'Angelica EC, Shotelersuk V, Aguilar RC, Gahl WA, Bonifacino JS. Altered trafficking of lysosomal membrane proteins in Hermansky–Pudlak syndrome due to mutations in the β3A subunit of the AP-3 adaptor complex. Mol Cell 1999;3:11–21.
5. Shotelersuk V, Dell'Angelica EC, Hartnell L, Bonifacino JS, Gahl WA. A new variant of Hermansky–Pudlak syndrome due to mutations in a gene responsible for vesicle formation. Am J Med 2000;108:423–427.
6. Robinson MS, Bonifacino JS. Adaptor-related proteins. Curr Opin Cell Biol 2001;13:444–453.
7. Oh J, Bailin T, Fukai K, Feng GH, Ho L, Mao JI, Frenk E, Tamura N, Spritz RA. Positional cloning of a gene for Hermansky–Pudlak syndrome, a disorder of cytoplasmic organelles. Nat Genet 1996;14:300–306.
8. Anikster Y, Huizing M, White J, Shevchenko YO, Fitzpatrick DL, Touchman JW, Compton JG, Bale SJ, Swank RT, Gahl WA, Toro JR. Mutation of a new gene causes a unique form of Hermansky–Pudlak syndrome in a genetic isolate of central Puerto Rico. Nat Genet 2001;28:376–380.
9. Suzuki T, Li W, Zhang Q, Karim A, Novak EK, Sviderskaya EV, Hill SP, Bennett DC, Levin AV, Nieuwenhuis HK, Fong CT, Castellan C, Miterski B, Swank B, Spritz RA. Hermansky–Pudlak syndrome is caused by mutations in HPS4, the human homolog of the mouse light-ear gene. Nat Genet 2002;30:321–324.
10. Swank RT, Novak EK, McGarry MP, Rusiniak ME, Feng L. Mouse models of Hermansky Pudlak syndrome: a review. Pigment Cell Res 1998;11:60–80.
11. Gardner JM, Wildenberg SC, Keiper NM, Novak EK, Rusiniak ME, Swank RT, Puri N, Finger JN, Hagiwara N, Lehman AL, Gales TL, Bayer ME, King RA, Brillant MH. The mouse pale ear (ep) mutation is the homologue of human Hermansky–Pudlak syndrome. Proc Natl Acad Sci USA 1997;94:9238–9243.
12. Feng GH, Bailin T, Oh J, Spritz RA. Mouse pale ear (*ep*) is homologous to human Hermansky–Pudlak syndrome and contains a rare 'AT-AC' intron. Hum Mol Genet 1997;6:793–797.
13. Feng L, Seymour AB, Jiang S, To A, Peden AA, Novak EK, Zhen L, Rusiniak ME, Eicher EM, Robinson MS et al. The beta3A subunit gene (Ap3b1) of the AP-3 adaptor complex is altered in the mouse hypopigmentation mutant pearl, a model for Hermansky–Pudlak syndrome and night blindness. Hum Mol Genet 1999;8:323–330.
14. Suzuki T, Li W, Zhang Q, Novak EK, Sviderskaya EV, Wilson A, Bennett DC, Roe BA, Swank RT, Spritz RA. The gene mutated in cocoa mice, carrying a defect of organelle biogenesis, is a homologue of the human Hermansky–Pudlak syndrome-3 gene. Genomics 2001;78:30–37.
15. Kantheti P, Qiao X, Diaz ME, Peden AA, Meyer GE, Carskadon SL, Kapfhamer D, Sufalko D, Robinson MS, Noebels JL, Burmeister M. Mutation in AP-3 delta in the mocha mouse links endosomal transport to storage deficiency in platelets, melanosomes, and synaptic vesicles. Neuron 1998;21:111–122.
16. Detter JC, Zhang Q, Mules EH, Novak EK, Mishra VS, Li W, McMurtrie EB, Tchernev VT, Wallace MR, Seabra MC et al. Rab geranylgeranyl transferase alpha mutation in the gunmetal mouse reduces Rab prenylation and platelet synthesis. Proc Natl Acad Sci USA 2000;97:4144–4149.
17. Huang L, Kuo Y-M, Gitschier J. The pallid gene encodes a novel, syntaxin 13-interacting protein involved in platelet storage pool deficiency. Nat Genet 1999;23:329–332.
18. Zhang Q, Li W, Novak EK, Karim A, Mishra VS, Kingsmore SF, Roe BA, Suzuki T, Swank RT. The gene for the muted (mu) mouse, a model for Hermansky–Pudlak syndrome, defines a novel protein which regulates vesicle trafficking. Hum Mol Genet 2002;11:697–706.
19. Seabra MC, Mules EH, Hume AN. Rab GTPases, intracellular traffic and disease. Trends Mol Med 2002;8:23–30.
20. McGarry MP, Reddington M, Novak EK, Swank RT. Survival and lung pathology of mouse models of Hermansky–Pudlak syndrome and Chediak–Higashi syndrome. Proc Soc Exp Biol Med 1999;220:162–168.
21. Lupas A. Coiled coils: new structures and new functions. Trends Biochem Sci 1996;21:375–382.
22. Dell'Angelica EC, Ooi CE, Bonifacino JS. β3A-adaptin, a subunit of the adaptor-like complex AP-3. J Biol Chem 1997;272:15078–15084.

23. Dell'Angelica EC, Ohno H, Ooi CE, Rabinovich E, Roche KW, Bonifacino JS. AP-3: an adaptor-like protein complex with ubiquitous expression. EMBO J 1997;15:917–928.
24. Dell'Angelica EC, Aguilar RC, Wolins N, Hazelwood S, Gahl WA, Bonifacino JS. Molecular characterization of the protein encoded by the Hermansky–Pudlak syndrome type 1 gene. J Biol Chem 2000;275:1300–1308.
25. Klausner RD, Lippincott-Schwartz J, Bonifacino JS. The T cell antigen receptor: insights into organelle biology. Annu Rev Cell Biol 1990;6:403–431.
26. Zhen L, Jiang S, Feng L, Bright NA, Peden AA, Seymour AB, Novak EK, Elliott R, Gorin MB, Robinson MS, Swank RT. Abnormal expression and subcellular distribution of subunit proteins of the AP-3 adaptor complex lead to platelet storage pool deficiency in the pearl mouse. Blood 1999;94:146–155.
27. Prekeris R, Klumperman J, Chen YA, Scheller RH. Syntaxin 13 mediates cycling of plasma membrane proteins via tubulovesicular recycling endosomes. J Cell Biol 1998;143:957–971.
28. Kirchhausen T. Clathrin. Annu Rev Biochem 2000;69:699–727.
29. Raposo G, Marks MS. The dark side of lysosome-related organelles: specialization of the endocytic pathway for melanosome biogenesis. Traffic 2002;3:237–248.
30. Raposo G, Tenza D, Murphy DM, Berson JF, Marks MS. Distinct protein sorting and localization to premelanosomes, melanosomes, and lysosomes in pigmented melanocytic cells. J Cell Biol 2001;152:809–824.
31. Le Borgne R, Alconada A, Bauer U, Hoflack B. The mammalian AP-3 adaptor-like complex mediates the intracellular transport of lysosomal membrane glycoproteins. J Biol Chem 1998;273:29451–29461.
32. Peden AA, Rudge RE, Lui WW, Robinson MS. Assembly and function of AP-3 complexes in cells expressing mutant subunits. J Cell Biol 2002;156:327–336.
33. Huizing M, Sarangarajan R, Strovel E, Zhao Y, Gahl WA, Boissy RE. AP-3 mediates tyrosinase but not TRP-1 trafficking in human melanocytes. Mol Biol Cell 2001;12:2075–2085.
34. Gwynn B, Ciciotte SL, Hunter SJ, Washburn LL, Smith RS, Andersen SG, Swank RT, Dell'Angelica EC, Bonifacino JS, Eicher EM, Peters LL. Defects in the cappuccino (cno) gene on mouse chromosome 5 and human 4p cause Hermansky–Pudlak syndrome by an AP-3-independent mechanism. Blood 2000;96:4227–4235.
35. TerBush DR, Maurice T, Roth D, Novick P. The Exocyst is a multiprotein complex required for exocytosis in *Saccharomyces cerevisiae*. EMBO J 1996;15:6483–6494.
36. Sacher M, Jiang Y, Barrowman J, Scarpa A, Burston J, Zhang L, Schieltz D, Yates JR, 3rd, Abeliovich H, Ferro-Novick S. TRAPP, a highly conserved novel complex on the cis-Golgi that mediates vesicle docking and fusion. EMBO J 1998;17:2494–2503.
37. Whyte JR, Munro S. The Sec34/35 Golgi transport complex is related to the exocyst, defining a family of complexes involved in multiple steps of membrane traffic. Dev Cell 2001;1:527–537.
38. Ungar D, Oka T, Brittle EE, Vasile E, Lupashin VV, Chatterton JE, Heuser JE, Krieger M, Waters MG. Characterization of a mammalian Golgi-localized protein complex, COG, that is required for normal Golgi morphology and function. J Cell Biol 2002;157:405–415.
39. Conibear E, Stevens TH. Vps52p, Vps53p, and Vps54p form a novel multisubunit complex required for protein sorting at the yeast late Golgi. Mol Biol Cell 2000;11:305–323.
40. Waters MG, Pfeffer SR. Membrane tethering in intracellular transport. Curr Opin Cell Biol 1999;11:453–459.
41. Falcon-Perez JM, Starcevic M, Gautam R, Dell'Angelica EC. BLOC-1, a novel complex containing the pallidin and muted proteins involved in the biogenesis of melanosomes and platelet dense granules. J Biol Chem 2002;in press:May 17 [epub ahead of print].